

# Extracting $\sigma_{\pi N}$ from pionic atoms\*

ELIAHU FRIEDMAN AND AVRAHAM GAL

Racah Institute of Physics, The Hebrew University  
Jerusalem 91904, Israel

We discuss a recent extraction of the  $\pi N$   $\sigma$  term  $\sigma_{\pi N}$  from a large-scale fit of pionic-atom strong-interaction data across the periodic table. The value thus derived,  $\sigma_{\pi N}^{\text{FG}} = 57 \pm 7$  MeV, is directly connected via the Gell-Mann–Oakes–Renner expression to the medium-renormalized  $\pi N$  isovector scattering amplitude near threshold. It compares well with the value derived recently by the Bern-Bonn-Jülich group,  $\sigma_{\pi N}^{\text{RS}} = 58 \pm 5$  MeV, using the Roy-Steiner equations to control the extrapolation of the vanishingly small near threshold  $\pi N$  isoscalar scattering amplitude to zero pion mass.

## 1. Introduction

The  $\pi N$   $\sigma$  term

$$\sigma_{\pi N} = \frac{\bar{m}_q}{2m_N} \sum_{u,d} \langle N | \bar{q}q | N \rangle, \quad \bar{m}_q = \frac{1}{2}(m_u + m_d), \quad (1)$$

sometimes called the nucleon  $\sigma$  term  $\sigma_N$ , records the contribution of explicit chiral symmetry breaking to the nucleon mass  $m_N$  arising from the non-zero value of the  $u$  and  $d$  quark masses in QCD. Early calculations yielded a wide range of values,  $\sigma_{\pi N} \sim (20 - 80)$  MeV [3]. Recent calculations use two distinct approaches: (i) pion-nucleon low-energy phenomenology guided by chiral EFT, with or without solving Roy-Steiner equations, result in values of  $\sigma_{\pi N} \sim (50 - 60)$  MeV [4, 5, 6, 7, 8], the most recent of which is  $58 \pm 5$  MeV; and (ii) lattice QCD (LQCD) calculations reach values of  $\sigma_{\pi N} \sim (30 - 50)$  MeV [9, 10, 11, 12, 13, 14, 15], the most recent of which is  $41.6 \pm 3.8$  MeV. This dichotomy is demonstrated on the left panel of Fig. 1. However, when augmented by chiral perturbation expansions, LQCD calculations reach also values of  $\sim 50$  MeV, see e.g. Refs. [16, 17, 18, 19]. Ambiguities in chiral extrapolations of LQCD calculations to the physical pion mass are demonstrated on the right panel of Fig. 1.

---

\* Presented in June 2019 at the 15th MENU Conf., Pittsburgh [1], and at the 3rd Jagiellonian Symposium on Fundamental and Applied Subatomic Physics, Kraków [2].

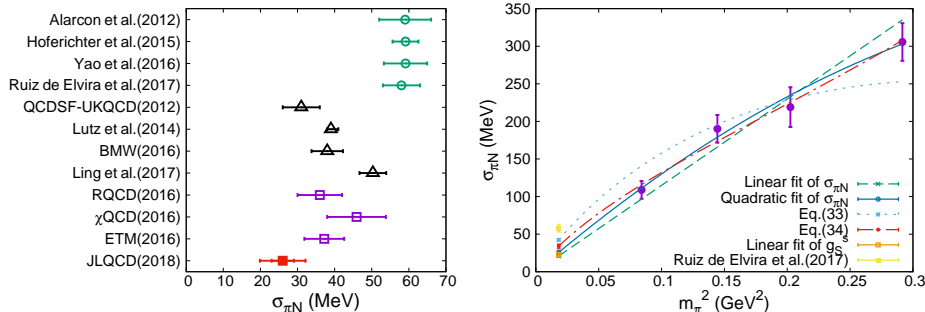


Fig. 1. Left: values of  $\sigma_{\pi N}$  from recent calculations, based on  $\pi N$  phenomenology (in green) and in LQCD (other colors). Right: chiral extrapolations of LQCD derived  $\sigma_{\pi N}$  values to the physical pion mass. Figure adapted from Ref. [14].

A third approach for evaluating  $\sigma_{\pi N}$  was recently proposed by us [20] focusing on the  $\sigma_{\pi N}$ -dependent in-medium renormalization of the  $\pi N$  isovector scattering length  $b_1$ , determined from a wealth of strong-interaction level shifts and widths data in pionic atoms across the periodic table [21]. This contrasts with extrapolating the vanishingly small  $\pi N$  isoscalar scattering length  $b_0$  from  $m_\pi \approx 138$  MeV to the Cheng-Dashen point or nearby at  $m_\pi \sim 0$ , as done in the first approach. To demonstrate the issues involved in comparing these two methodologies, we cite from a recent work by the Bern-Bonn-Jülich group [22] an expression relating the expected departure of the evaluated  $\sigma_{\pi N}$  from their value of  $59 \pm 3$  MeV [6] upon varying the input values of  $b_0$  and  $b_1$ :

$$\sigma_{\pi N} \approx (59 \pm 3) \text{ MeV} + 1.116 \Delta b_0^{\text{free}} + 0.390 \Delta b_1^{\text{free}}, \quad (2)$$

where  $\Delta b_j^{\text{free}}$ ,  $j = 0, 1$ , is the difference between the values of  $b_j^{\text{free}}$  (in units of  $10^{-3} m_\pi^{-1}$ ) used in a given specific model and those used in the calculation of Ref. [6]. Eq. (2) suggests that the uncertainty in the determination of  $\sigma_{\pi N}$  incurred by the model dependence of  $b_0^{\text{free}}$  is roughly three times larger than that incurred by the model dependence of  $b_1^{\text{free}}$ . Regarding the model dependence of these free-space scattering lengths we note the two sets of input scattering lengths ( $b_0^{\text{free}}, b_1^{\text{free}}$ ) discussed in Ref. [22],

$$(-0.9, -85.3) \times 10^{-3} m_\pi^{-1}, \quad (+7.9, -85.4) \times 10^{-3} m_\pi^{-1}, \quad (3)$$

differing from each other by whether or not charge dependent effects are incorporated into the values of scattering lengths derived from  $\pi^- \text{H}$  and  $\pi^- \text{d}$  atoms by Baru *et al.* [23]. It is evident that the charge dependence of the near threshold  $\pi N$  interaction affects dominantly the isoscalar  $b_0^{\text{free}}$  while

leaving the isovector  $b_1^{\text{free}}$  basically intact. This makes an approach based on  $b_1^{\text{free}}$  quite attractive.

To set the stage for how the third approach works we note that the  $\pi N$  scattering lengths [23] are well approximated by the Tomozawa-Weinberg leading-order (LO) chiral limit [24]

$$b_0^{\text{LO}} = 0, \quad b_1^{\text{LO}} = -\frac{\mu_{\pi N}}{8\pi f_\pi^2} = -79 \times 10^{-3} m_\pi^{-1}, \quad (4)$$

where  $\mu_{\pi N}$  is the  $\pi N$  reduced mass and  $f_\pi = 92.2$  MeV is the free-space pion decay constant. This expression for the isovector amplitude  $b_1$  suggests that its in-medium renormalization is directly connected to that of  $f_\pi$ , given to first order in the nuclear density  $\rho$  by the Gell-Mann - Oakes - Renner (GMOR) expression [25]

$$\frac{f_\pi^2(\rho)}{f_\pi^2} = \frac{\langle \bar{q}q \rangle_\rho}{\langle \bar{q}q \rangle} \simeq 1 - \frac{\sigma_{\pi N}}{m_\pi^2 f_\pi^2} \rho, \quad (5)$$

where  $\langle \bar{q}q \rangle_\rho$  stands for the in-medium quark condensate. The decrease of  $\langle \bar{q}q \rangle_\rho$  with density in Eq. (5) marks the leading low-density behavior of the order parameter of the spontaneously broken chiral symmetry, see e.g. Ref. [26]. Recalling the  $f_\pi$  dependence of  $b_1^{\text{LO}}$  in Eq. (4), Eq. (5) suggests the following density dependence for the in-medium  $b_1$ :

$$b_1 = b_1^{\text{free}} \left( 1 - \frac{\sigma_{\pi N}}{m_\pi^2 f_\pi^2} \rho \right)^{-1}. \quad (6)$$

In this model, introduced by Weise [27, 28], the explicitly density-dependent  $b_1(\rho)$  of Eq. (6) figures directly in the pion-nucleus  $s$ -wave near-threshold potential. Studies of pionic atoms [29] and low-energy pion-nucleus scattering [30, 31] confirmed that the  $\pi N$  isovector  $s$ -wave interaction term is indeed renormalized in agreement with Eq. (6). It is this in-medium renormalization that brings in  $\sigma_{\pi N}$  to the interpretation of pionic-atom data. However, the value of  $\sigma_{\pi N}$  was held fixed around 50 MeV in these studies, with no attempt to determine its optimal value.

In our recent work [20] we kept to the  $\pi N$  isovector  $s$ -wave amplitude  $b_1$  renormalization given by Eq. (6), but varied also  $\sigma_{\pi N}$  in fits to a comprehensive set of pionic atoms data across the periodic table. Other real  $\pi N$  interaction parameters varied together with  $\sigma_{\pi N}$  converged at expected free-space values. Holding these parameters fixed at the converged values, except for the tiny isoscalar  $s$ -wave single-nucleon amplitude  $b_0$  which is renormalized primarily by a double-scattering term (see below), we obtained a best-fit value of  $\sigma_{\pi N}^{\text{FG}} = 57 \pm 7$  MeV. A more comprehensive discussion of our fits to pionic atoms data is provided here. The pionic atoms approach used by us to extract  $\sigma_{\pi N}$  is reviewed in the next section, followed by results and discussion in subsequent sections.

## 2. Pionic atoms optical potentials

The starting point in our most recent optical-potential analysis of pionic atoms [29] is the in-medium pion self-energy  $\Pi(E, \vec{p}, \rho)$  that enters the in-medium pion dispersion relation

$$E^2 - \vec{p}^2 - m_\pi^2 - \Pi(E, \vec{p}, \rho) = 0, \quad (7)$$

where  $\vec{p}$  and  $E$  are the pion momentum and energy, respectively, in nuclear matter of density  $\rho$ . The resulting pion-nuclear optical potential  $V_{\text{opt}}$ , defined by  $\Pi(E, \vec{p}, \rho) = 2EV_{\text{opt}}$ , enters the near-threshold pion wave equation

$$[\nabla^2 - 2\mu(B + V_{\text{opt}} + V_c) + (V_c + B)^2] \psi = 0, \quad (8)$$

where  $\hbar = c = 1$ . Here  $\mu$  is the pion-nucleus reduced mass,  $B$  is the complex binding energy,  $V_c$  is the finite-size Coulomb interaction of the pion with the nucleus, including vacuum-polarization terms, all added according to the minimal substitution principle  $E \rightarrow E - V_c$ . Interaction terms negligible with respect to  $2\mu V_{\text{opt}}$ , i.e.  $2V_c V_{\text{opt}}$  and  $2B V_{\text{opt}}$ , are omitted. We use the Ericson-Ericson form [32]

$$2\mu V_{\text{opt}}(r) = q(r) + \vec{\nabla} \cdot \left( \frac{\alpha_1(r)}{1 + \frac{1}{3}\xi\alpha_1(r)} + \alpha_2(r) \right) \vec{\nabla}, \quad (9)$$

with  $s$ -wave part  $q(r)$  and  $p$ -wave part,  $\alpha_1(r)$  and  $\alpha_2(r)$ , given by [21]

$$\begin{aligned} q(r) = & -4\pi\left(1 + \frac{\mu}{m_N}\right)\{b_0[\rho_n(r) + \rho_p(r)] + b_1[\rho_n(r) - \rho_p(r)]\} \\ & -4\pi\left(1 + \frac{\mu}{2m_N}\right)4B_0\rho_n(r)\rho_p(r), \end{aligned} \quad (10)$$

$$\alpha_1(r) = 4\pi\left(1 + \frac{\mu}{m_N}\right)^{-1}\{c_0[\tilde{\rho}_n(r) + \tilde{\rho}_p(r)] + c_1[\tilde{\rho}_n(r) - \tilde{\rho}_p(r)]\}, \quad (11)$$

$$\alpha_2(r) = 4\pi\left(1 + \frac{\mu}{2m_N}\right)^{-1}4C_0\tilde{\rho}_n(r)\tilde{\rho}_p(r), \quad (12)$$

augmented by  $p$ -wave angle-transformation terms of order  $O(m_\pi/m_N)$ . Here  $\rho_n$  and  $\rho_p$  are neutron and proton density distributions normalized to the number of neutrons  $N$  and number of protons  $Z$ , respectively, and  $\tilde{\rho}_n$  and  $\tilde{\rho}_p$  are obtained from  $\rho_n$  and  $\rho_p$  by folding a  $\pi N\Delta$  form factor [33]. The coefficients  $b_0$ ,  $b_1$  in Eq. (10) are effective density-dependent pion-nucleon isoscalar and isovector  $s$ -wave scattering amplitudes, respectively, evolving from the free-space scattering lengths, and are essentially real near threshold. Similarly, the coefficients  $c_0$ ,  $c_1$  in Eq. (11) are effective  $p$ -wave scattering amplitudes which, since the  $p$ -wave part of  $V_{\text{opt}}$  acts mostly near the

nuclear surface, are close to the free-space scattering volumes provided  $\xi = 1$  is applied in the Lorentz-Lorenz renormalization of  $\alpha_1$  in Eq. (9). The parameters  $B_0$  and  $C_0$  represent multi-nucleon absorption and therefore have an imaginary part. Their real parts stand for dispersive contributions which often are absorbed into the respective single-nucleon amplitudes [34]. Below we focus on the  $s$ -wave part  $q(r)$  of  $V_{\text{opt}}$ .

Regarding the isoscalar amplitude  $b_0$ , since the free-space value  $b_0^{\text{free}}$  is exceptionally small, it is customary in the analysis of pionic atoms to supplement it by double-scattering contributions induced by Pauli correlations. For completeness we also include similar contributions to  $b_1$  which decrease its value, although by only less than 10%. Thus, the single-nucleon  $b_0$  and  $b_1$  terms in Eq. (10) are extended to account also for double-scattering [32, 35],

$$\tilde{b}_0 \rightarrow \tilde{b}_0 - \frac{3}{2\pi} (\tilde{b}_0^2 + 2\tilde{b}_1^2) p_F, \quad \tilde{b}_1 \rightarrow \tilde{b}_1 + \frac{3}{2\pi} (\tilde{b}_1^2 - 2\tilde{b}_0\tilde{b}_1) p_F, \quad (13)$$

where  $\tilde{b}_j \equiv (1 + \frac{m_\pi}{m_N})b_j$ , and  $p_F$  is the local Fermi momentum corresponding to the local nuclear density  $\rho = 2p_F^3/(3\pi^2)$ .

Regarding the isovector amplitude  $b_1$ , it affects primarily level shifts in pionic atoms with  $N - Z \neq 0$ . However, it affects also  $N = Z$  pionic atoms through the dominant quadratic  $b_1$  contribution to  $b_0$  of Eq. (13). This dominance follows already at the level of  $b_1^{\text{free}}$  from a systematic expansion of the pion self-energy up to  $O(p^4)$  in nucleon and pion momenta within chiral perturbation theory [36]. Following Ref. [37] it can be argued that it is the in-medium  $b_1$  Eq. (6) that enters the Pauli-correlation double-scattering contribution in Eq. (13). This approach has been practised in numerous global fits to pionic atoms by us [21, 29] as well as by other groups, e.g. Geissel et al. [38], using a fixed value of  $\sigma_{\pi N}$ . To study the role of a variable  $\sigma_{\pi N}$  as per Eq. (6) we extended  $b_1$  wherever appearing in Eq. (13) by substituting

$$b_1 \rightarrow b_1 \left( 1 - \frac{\sigma_{\pi N}}{m_\pi^2 f_\pi^2 \rho} \right)^{-1}. \quad (14)$$

Regarding the nuclear densities  $\rho_p$  and  $\rho_n$  that enter the potential, Eqs. (10)–(12), two-parameter Fermi distributions with the same diffuseness parameter for protons and neutrons were used [21, 39] yielding lower values of  $\chi^2$  than other shapes do for pions. With proton densities determined from nuclear charge densities, the neutron densities were varied, searching for best agreement with the pionic atoms data by assuming a linear dependence of  $r_n - r_p$ , the difference between the root-mean-square (rms) radii, on the neutron excess ratio  $(N - Z)/A$ :

$$r_n - r_p = \gamma \frac{N - Z}{A} + \delta, \quad (15)$$

with  $\gamma$  close to 1.0 fm and  $\delta$  close to zero. Here we used  $\delta = -0.035$  fm and varied  $\gamma$ . For example,  $\gamma=1$  fm means  $r_n - r_p = 0.177$  fm in  $^{208}\text{Pb}$ , a value compatible with several analyses of pion strong and electromagnetic interactions in  $^{208}\text{Pb}$  [40, 41], and with other determinations of the so called ‘neutron skin’.

### 3. Results

Following the optical potential approach described in the preceding section, and more extensively in Refs. [21, 29], global fits to strong interaction level shifts and widths from Ne to U were made over a wide range of values for the neutron-skin parameter  $\gamma$  as shown in Fig. 2.

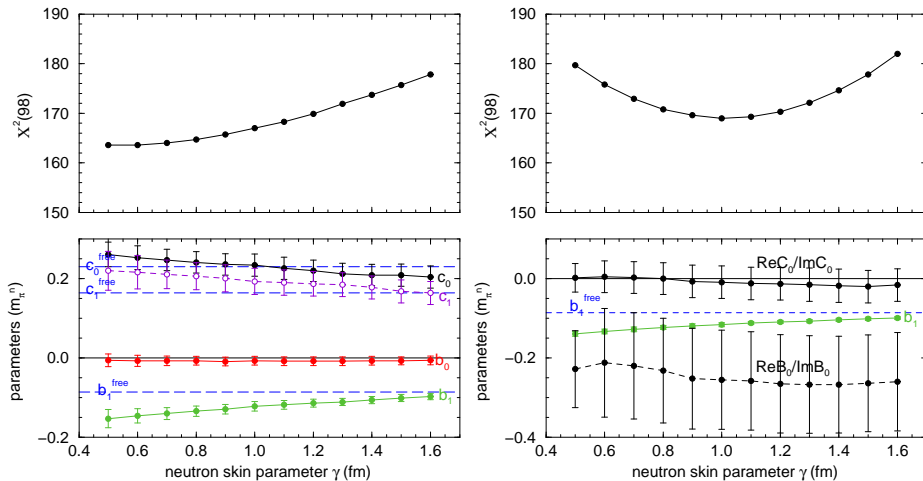


Fig. 2. Fits to 98 pionic atoms data points for  $\sigma_{\pi N} = 0$  as a function of the neutron-skin parameter  $\gamma$ , with  $\chi^2$  values plotted in the upper panels and fitted values of some of the  $\pi$ -nucleus optical potential parameters plotted in the lower panels. No  $\chi^2$  minimum is reached in the 8-parameter left-panel fits, but fixing the  $p$ -wave parameters  $c_0$  and  $c_1$  at their SAID [42] threshold values  $0.23$  and  $0.16 m_\pi^{-3}$ , respectively, produces the fits shown in the right panels.

The fitted 98 data points include ‘deeply bound’ states in Sn isotopes and in  $^{205}\text{Pb}$ . Varying all eight parameters (real  $b_0$ ,  $b_1$ ,  $c_0$ ,  $c_1$ ; complex  $B_0$ ,  $C_0$ ) in Eqs. (10)–(12) produces good  $\chi^2$  fits,  $\chi^2 \sim 170$ , but short of a well defined  $\chi^2(\gamma)$  minimum as clearly seen in the upper left panel of Fig. 2. The lower left panel shows that the single-nucleon parameters are well determined and vary smoothly with  $\gamma$ .

Holding the  $p$ -wave single-nucleon parameters  $c_0, c_1$  fixed at their SAID free-space threshold values marked by dashed horizontal lines, thereby reducing the number of fitted parameters to six, a  $\chi^2$  minimum around  $\gamma = 1$  to 1.1 fm was reached as shown in the upper right panel of Fig. 2. In these six-parameter fits,  $\text{Im } B_0$  and  $\text{Im } C_0$  (not shown) come out well-determined, with values almost independent of  $\gamma$ , but  $\text{Re } B_0$  and  $\text{Re } C_0$  are poorly determined as seen in the lower right panel of the figure. In all the fits shown here in Fig. 2,  $b_1$  was treated as a free parameter regardless of any possible functional dependence on  $\sigma_{\pi N}$ , thereby corresponding to  $\sigma_{\pi N} = 0$  in Eq. (14). The fitted values of  $b_1$  disagree then over a broad range of  $\gamma$ s with the value  $b_1^{\text{free}}$  marked by a dashed horizontal line.

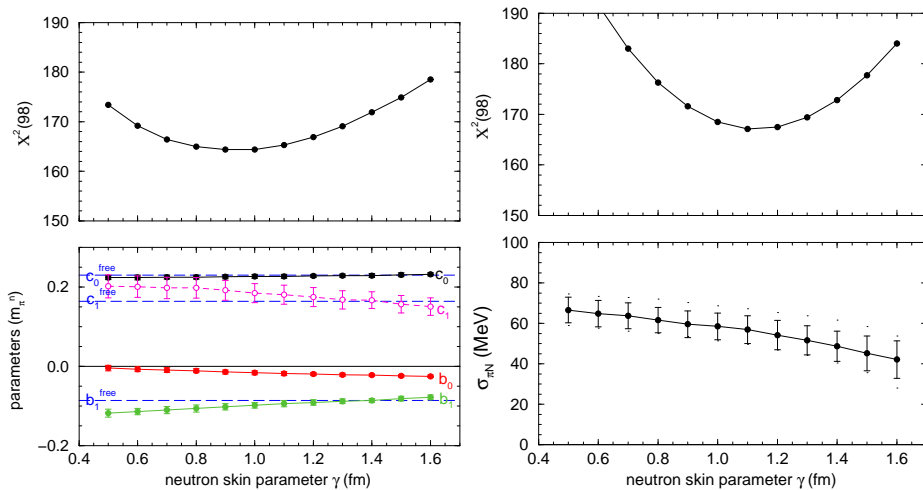


Fig. 3. Left: 6-parameter fits with  $\sigma_{\pi N} = 50$  MeV where  $\text{Re } B_0$  and  $\text{Re } C_0$  are kept zero. Right: 4-parameter fits where  $c_0$  and  $c_1$ , additionally, are kept at their SAID [42] threshold values  $0.23$  and  $0.16 m_\pi^{-3}$ , respectively. Of the 4 varied parameters ( $b_0, b_1, \text{Im } B_0, \text{Im } C_0$ )  $b_1$  is related to  $\sigma_{\pi N}$  by Eq. (6). Resulting values of  $\sigma_{\pi N}$  are plotted in the lower right panel.

Introducing the in-medium density dependence of  $b_1$  given by Eq. (14) in terms of  $\sigma_{\pi N}$  we first demonstrate the effect of using a fixed value of  $\sigma_{\pi N} = 50$  MeV, as practised in all of our past works [29], on the fitted parameters. This is shown within six-parameter fits in the left panels of Fig. 3. Rather than keeping the  $p$ -wave single-nucleon parameters  $c_0$  and  $c_1$  to their SAID free-space threshold values, as done in the  $\sigma_{\pi N} = 0$  fits shown in the right panels of Fig. 2, here we kept  $\text{Re } B_0$  and  $\text{Re } C_0$  to zero values thereby producing as good fits to the data as by letting them vary.

In particular, suppressing  $\text{Re } B_0$  in pionic atoms fits amounts to absorbing it into an effective  $b_0$  parameter [34]. The fitted  $c_0$  and  $c_1$ , particularly  $c_0$ , are clearly seen in the lower panel to come out close to the respective free-space values. As for the  $s$ -wave single-nucleon parameters  $b_0$  and  $b_1$ , the dominance of  $b_1$  with respect to  $b_0$  is also clearly seen. The introduction of a nonzero value of  $\sigma_{\pi N}$  allows  $b_1$  to reach its free-space value  $b_1^{\text{free}}$  beginning at a neutron-skin parameter  $\gamma$  value of 1.1 fm.

Holding now the  $p$ -wave single-nucleon parameters  $c_0$  and  $c_1$  at their free-space SAID threshold values 0.23 and 0.16  $m_\pi^{-3}$ , respectively, and keeping as before  $\text{Re } B_0$  and  $\text{Re } C_0$  to zero values, we show in the right panels of Fig. 3 four-parameter fits where the varied parameters are  $b_0$ ,  $\sigma_{\pi N}$  for  $b_1$  using Eq. (6),  $\text{Im } B_0$  and  $\text{Im } C_0$ . A minimum value of  $\chi^2_{\text{min}} = 167.1$  is reached at  $\gamma \approx 1.1$  fm where  $\sigma_{\pi N}$  assumes a value of  $\sigma_{\pi N}^{\text{FG}} = 56.9 \pm 6.9$  MeV. Note that a value of  $\gamma \approx 1.1$  fm agrees with other determinations of this quantity in  $^{208}\text{Pb}$  [41]. To check the dependence of  $\sigma_{\pi N}$  on  $b_0$  we repeated fits with  $b_0$  kept fixed at either one of the two free-space threshold values listed in Eq. (3), varying then also  $\text{Re } B_0$  and  $\text{Re } C_0$ . Typical  $\chi^2$  values increased by 20 to 30, but the  $\chi^2$  minima remained at  $\gamma = 1.1$  to 1.2 fm with corresponding values of  $\sigma_{\pi N}$  decreasing at most by 3 MeV. We also note that the resulting value of  $\sigma_{\pi N}$  is identical with that derived in our recently published work [20] where the effect on the derived value of  $\sigma_{\pi N}$  of form-factor folding,  $\rho_{n,p} \rightarrow \tilde{\rho}_{n,p}$  in the  $p$ -wave terms (11,12) of the pion-nucleus optical potential, was shown to be negligibly small.

#### 4. Discussion and summary

The pionic atoms fits and the value of the  $\pi N$   $\sigma$  term  $\sigma_{\pi N}$  extracted in the present work are based on the in-medium renormalization of the near-threshold  $\pi N$  isovector scattering amplitude  $b_1$  as given by Eq. (6), derived at LO from Eqs. (4) and (5) for the in-medium decrease of the pion decay constant  $f_\pi$  associated via the GMOR expression with the in-medium decrease of the quark condensate  $\langle \bar{q}q \rangle$ . Higher order corrections to this simple form have been proposed in the literature and were discussed by us in Ref. [20]. Briefly, one may classify two such corrections arising from: (i)  $NN$  correlation contributions [43] from one- and two-pion interaction terms, increasing the fitted  $\sigma_{\pi N}$  value by about 7 MeV (or by a smaller amount following a chiral approach at NLO [44]); and (ii) an upward shift of the in-medium pion mass  $m_\pi(\rho)$  in symmetric nuclear matter from its free-space value [45], decreasing the fitted  $\sigma_{\pi N}$  value by a similar amount, and also by adding corrections of order  $\rho^{4/3}$  [46, 47] which at a typical nuclear density  $\rho_{\text{eff}} = 0.1 \text{ fm}^{-3}$  [34] are negligible. Interestingly but perhaps fortuitously, these two higher-order effects largely cancel each other.

In conclusion, we have derived in this work a value of  $\sigma_{\pi N}^{\text{FG}} = 57 \pm 7$  MeV from a large scale fit to pionic atoms observables, in agreement with the relatively high  $\sigma_{\pi N}$  values reported in recent studies based on modern hadronic  $\pi N$  phenomenology [8], but in disagreement with the considerably lower  $\sigma_{\pi N}$  values reached in some of the recent modern lattice QCD calculations, e.g. [14]. Our derivation is based on the model introduced by Weise and collaborators [27, 28, 37] for the in-medium renormalization of the  $\pi N$  near-threshold isovector scattering amplitude, using its leading density dependence Eq. (6), and was found robust in fitting the wealth of pionic atoms data against variation of other  $\pi N$  interaction parameters that enter the low-energy pion self-energy operator. The two types of model corrections beyond the leading density dependence considered here were found to be relatively small, a few MeV each, and partly canceling each other. Further model studies are desirable in order to confirm this conclusion.

### Acknowledgments

We are grateful to Norbert Kaiser, Wolfram Weise and Nodoka Yamanaka for useful correspondence on the subject of the present work.

### REFERENCES

- [1] E. Friedman, A. Gal, AIP Conf. Proc. **2249**, 030015 (2020).
- [2] E. Friedman, A. Gal, Acta Phys. Pol. B **51**, 45 (2020).
- [3] M.E. Sainio,  $\pi N$  Newsletter **16**, 138 (2002) [arXiv:hep-ph/0110413].
- [4] J.M. Alarcón, J.M. Camalich, J.A. Oller, Phys. Rev. D **85**, 051503 (2012).
- [5] Y.-H. Chen, D.-L. Yao, H.Q. Zheng, Phys. Rev. D **87**, 054019 (2013).
- [6] M. Hoferichter, J. Ruiz de Elvira, B. Kubis, U.-G. Meißner, Phys. Rev. Lett. **115**, 092301 (2015).
- [7] V. Dmitrašinović, H.-X. Chen, A. Hosaka, Phys. Rev. C **93**, 065208 (2016).
- [8] J. Ruiz de Elvira, M. Hoferichter, B. Kubis, U.-G. Meißner, J. Phys. G **45**, 024001 (2018).
- [9] R. Horsley *et al.* (QCDSF-UKQCD Collab.), Phys. Rev. D **85**, 034506 (2012).
- [10] S. Durr *et al.* (BMW Collab.), Phys. Rev. Lett. **116**, 172001 (2016).
- [11] Y.-B. Yang, A. Alexandru, T. Draper, K.-F. Liu ( $\chi$ QCD Collab.), Phys. Rev. D **94**, 054503 (2016).
- [12] A. Abdel-Rehim *et al.* (ETM Collab.), Phys. Rev. Lett. **116**, 252001 (2016).
- [13] G.S. Bali *et al.* (RQCD Collab.), Phys. Rev. D **93**, 094504 (2016).
- [14] N. Yamanaka, S. Hashimoto, T. Kaneko, H. Ohki (JLQCD Collab.), Phys. Rev. D **98**, 054516 (2018).

- [15] C. Alexandrou *et al.* (ETM Collab.), arXiv:1909.00485v1.
- [16] D.B. Leinweber, A.W. Thomas, S.V. Wright, Phys. Lett. B **482**, 109 (2000).
- [17] L. Alvarez-Ruso, T. Ledwig, J.M. Camalich, M.J. Vicente-Vacas, Phys. Rev. D **88**, 054507 (2013).
- [18] X.-L. Ren, L.-S. Geng, J. Meng, Phys. Rev. D **91**, 051502(R) (2015).
- [19] X.-L. Ren, X.-Z. Ling, L.-S. Geng, Phys. Lett. B **783**, 7 (2018).
- [20] E. Friedman, A. Gal, Phys. Lett. **792**, 340 (2019).
- [21] E. Friedman, A. Gal, Phys. Rep. **452**, 89 (2007).
- [22] M. Hoferichter, J. Ruiz de Elvira, B. Kubis, U.-G. Meißner, Phys. Lett. B **760**, 74 (2016).
- [23] V. Baru *et al.*, Phys. Lett. B **694**, 473 (2011); Nucl. Phys. A **872**, 69 (2011).
- [24] Y. Tomozawa, Nuovo Cim. A **46**, 707 (1966); S. Weinberg, Phys. Rev. Lett. **17**, 616 (1966).
- [25] M. Gell-Mann, R.J. Oakes, B. Renner, Phys. Rev. **175**, 2195 (1968).
- [26] T.D. Cohen, R.J. Furnstahl, D.K. Griegel, Phys. Rev. C **45**, 1881 (1992).
- [27] W. Weise, Acta Phys. Pol. B **31**, 2715 (2000).
- [28] W. Weise, Nucl. Phys. A **690**, 98c (2001).
- [29] E. Friedman, A. Gal, Nucl. Phys. A **928**, 128 (2014), and references therein to earlier work on pionic atoms.
- [30] E. Friedman *et al.*, Phys. Rev. Lett. **93**, 122302 (2004).
- [31] E. Friedman *et al.*, Phys. Rev. C **72**, 034609 (2005).
- [32] M. Ericson, T.E.O. Ericson, Ann. Phys. **36**, 323 (1966).
- [33] A. Gal, H. Garcilazo, Nucl. Phys. A **864**, 153 (2011); see Fig. 2 & Tab. 3.
- [34] R. Seki, K. Masutani, Phys. Rev. C **27**, 2799 (1983).
- [35] M. Krell, T.E.O. Ericson, Nucl. Phys. B **11**, 521 (1969).
- [36] N. Kaiser, W. Weise, Phys. Lett. B **512**, 283 (2001).
- [37] E.E. Kolomeitsev, N. Kaiser, W. Weise, Phys. Rev. Lett. **90**, 092501 (2003).
- [38] H. Geissel *et al.*, Phys. Lett. B **549**, 64 (2002); Phys. Rev. Lett. **88**, 122301 (2002).
- [39] E. Friedman, Hyperfine Interact. **193**, 33 (2009).
- [40] E. Friedman, Nucl. Phys. A **896**, 46 (2012).
- [41] C.M. Tarbert *et al.*, Phys. Rev. Lett. **112**, 242502 (2014).
- [42] R.A. Arndt, W.J. Briscoe, I.I. Strakovsky, R.L. Workman, Phys. Rev. C **74**, 045205 (2006); evolving SAID program <http://gwdac.phys.gwu.edu/>
- [43] N. Kaiser, P. de Homont, W. Weise, Phys. Rev. C **77**, 025204 (2008).
- [44] A. Lacour, J.A. Oller, U.-G. Meißner, J. Phys. G **37**, 125002 (2010).
- [45] D. Jido, T. Hatsuda, T. Kunihiro, Phys. Lett. B **670**, 109 (2008).
- [46] S. Goda, D. Jido, Phys. Rev. C **88**, 065204 (2013).
- [47] S. Goda, D. Jido, Prog. Theor. Exp. Phys. **2014**, 033D03 (2014).